DEVELOPMENT OF NONLINEAR ANALYSIS OF LARGE-SCALE AXI-SYMMETRIC REINFORCED CONCRETE STRUCTURES

Taweep Chaisomphob

Department of Civil Engineering,

Sirindhorn International Institute of Technology, Thammasat University, Thailand.

ABSTRACT

The paper presents the theoretical development of numerical procedure to perform a nonlinear finite element analysis of axi-symmetric reinforced concrete structures. The developed constitutive model for a nonlinear axi-symmetric reinforced concrete element is based on the smeared crack concept with a simplification that after cracking of concrete the behaviors of two-dimensional and one-dimensional stress states are considered separately, and the model of cracked element is constructed by the superposition between the two-dimensional and one-dimensional models. The verification of the newly developed model is made by comparing with the tested circular slab under a uniformly distributed load. The applicability of the proposed nonlinear procedure to the problems of large-scale axi-symmetric reinforced concrete structures is confirmed by a good agreement between the numerical and experimental results of the massive reinforced concrete slab of 7 meter thickness.

Key Words: *axi-symmetric, nonlinear analysis, reinforced concrete, slab*

1. INTRODUCTION

Finite element method is widely used for the nonlinear structural analysis due to its efficiency. In the fields of reinforced concrete structures, a large number of researches on two-dimensional model were reported, however, a few studies on three-dimensional model applied to axi-symmetric structures were performed [1]. For example, Cheung, et al. [2], Rangan [3], Shehata, et al [4], Zhou, et al [5] proposed the various methods to predict the behaviour of reinforced concrete slabs. Extensive experimental investigation on the reinforced concrete circular slab subjected to a uniformly distributed load was performed by Iwaki, et al. [6].

In this paper, the simplified constitutive models for axi-symmetric reinforced concrete structures are developed by the superposition between the two-dimensional model and one-dimensional model in the range of concrete cracking. For each of the models, the Okamura and Maekawa's models [7] are utilized due to their reliability verified by several experimental

results. The proposed models are implemented into the "WCOMR" (Reinforced Concrete Model for Walls Subjected to Reversed Cyclic Load) developed by Okamura and Maekawa [7]. In order to demonstrate the validity of the proposed models, the results of the test of circular slabs under a uniformly distributed load by Iwaki et. al. [6] are compared with those of the present numerical analyses. In addition, the full-scale test results on the massive bottom slab of the liquefied natural gas (LNG) inground storage tank are compared with the numerical results.

2. THEORETICAL DEVELOPMENT

Based on a smeared crack model dealing macroscopically with cracked concretes and reinforcing bars by expressing the average stress and average strain relationships in a reinforced concrete (RC) element, Okamua and Maekawa established a constitutive model for the cracked concrete, and the nonlinear finite element program called WCOMR was developed to analyze the reinforced concrete panel structure [7]. The reliability of Okamura and Maekawa's constitutive model was verified with a large number of experimental results. In this study, this Okamura and Maekawa's constitutive model is selected. In order to apply this model for the problem of axi-symmetric RC structures, the model has to be modified to meet the axi-symmetric stress state as described below.

2.1 Model before cracking

For the constitutive model of axi-symmetric reinforced concrete element in the elastic range, i.e., before cracking of concrete, the material is assumed to follow linear elastic constitutive model. The stress-strain relation for a linear elastic axi-symmetric material is expressed by

$$\begin{Bmatrix} \sigma_{rr} \\ \sigma_{zz} \\ \tau_{rz} \\ \sigma_{\theta\theta} \end{Bmatrix} = \frac{1}{(1+\nu)(1-2\nu)} \begin{bmatrix} (1-\nu)E_c & \nu E_c & 0 & \nu E_c \\ & (1-\nu)E_c & 0 & \nu E_c \\ Symmetry & & \frac{(1-2\nu)}{2}E_c & 0 \\ & & & (1-\nu)E_c \end{bmatrix} \begin{Bmatrix} \varepsilon_{rr} \\ \varepsilon_{zz} \\ \gamma_{rz} \\ \varepsilon_{\theta\theta} \end{Bmatrix} \quad (1)$$

where σ_{rr}, σ_{zz}, τ_{rz} are axial stresses in r-direction (radial) and z-direction (vertical), and shear stress in rz plane; ε_{rr}, ε_{zz}, γ_{rz} are corresponding strains; $\sigma_{\theta\theta}$, $\varepsilon_{\theta\theta}$ are stress and strain in θ-direction (hoop) (see Fig.1); E_c, ν are modulus of elasticity and Poisson' s ratio of concrete. It is noted that stiffnesses of reinforcing bars are excluded in the above equation due to their negligible effects in comparison with those of concrete.

2.2 Model after cracking

In the present model, after cracking in either of three directions, i.e., radial, vertical or hoop direction, the material is assumed to behave separately in the plane of radial and vertical direction and in the hoop direction. In other words, it is assumed that there are no coupling effects between the behavior in the plane of radial and vertical direction and that in the hoop direction (see Fig.1). From the above consideration, the constitutive model for axi-symmetric cracked RC element can be divided into two independent models, i.e., 2-dimensional model in the plane of radial and vertical direction (σ_{rr}, σ_{zz}, τ_{rz} in Fig.1) and 1-dimensional model in the hoop direction ($\sigma_{\theta\theta}$ in Fig. 1).

2.2.1 Two-dimensional model

For 2-dimensional model, the constitutive model developed by Okamura and Maekawa [7] is adopted. In their model, the cracked RC element has been constructed by combining the constitutive law for cracked concrete and that for reinforcing bars (Fig.2a), in which the relationships between the average stress and the average strain are given. In the constitutive

law for the cracked concrete, there are three independent models namely (Fig. 2b):

- Tension stiffening model for tensile stress-strain in the direction perpendicular to the crack
- Compression model for compressive stress-strain in the direction parallel to the crack
- Shear transfer model for shear stress-strain along the crack

The details of formulation of the constitution law can be found in Ref. [7].

2.2.2 One-dimensional model

For 1-dimensional model, the original constitutive laws developed by Okamura and Maekawa based on uniaxial test of RC element under tension and compression are employed as follows;

(a) Uniaxial tensile stress-strain relationship

From Ref. [7], [8], [9], when cracks occur in the RC element under uniaxial tension, the average stress-strain relationship for the bar in concrete has been formulated by assuming the tensile stress distribution of the bar as a consine curve (Fig. 3a), and the tension stiffening model of the concrete (Fig. 3b). Examples of the average stress-strain relation of bar in concrete are shown in Fig.3c. By combining the average stress-strain relation of concrete (Fig.3b) and bar (Fig.3c), that of RC can be obtained.

(b) Uniaxial compressive stress-strain relationship

In Ref. [7], [10], [11], the relationship between average stress and strain for cracked concrete under compression is expressed by (Fig.4)

$$\sigma'_c = E_0 K (\varepsilon'_c - \varepsilon'_p) \quad (2)$$

where

$$E_0 = \frac{2f''_c}{\varepsilon'_{c0}} \quad (3)$$

$$K = \exp\left[-0.73\left(\frac{\varepsilon'_c}{\varepsilon'_{c0}}\right)\left\{1-\exp\left(-1.25\,\frac{\varepsilon'_c}{\varepsilon'_{c0}}\right)\right\}\right] \quad (4)$$

$$\varepsilon'_p = \varepsilon'_c - \varepsilon'_{c0}\left(\frac{20}{7}\right)\left\{1-\exp\left(-\frac{0.35\varepsilon'_c}{\varepsilon'_{c0}}\right)\right\} \quad (5)$$

in which E_0, K, ε'_p are called initial tangential elastic constant, fracture parameter, plastic compressive strain, respectively; f_c'': uniaxial compressive strength of concrete; ε'_{c0} : compressive strain corresponding to f_c'', ε'_{c0} = 0.15%-0.25% σ'_c, ε'_c : compressive stress and strain of concrete, respectively.

For the model of bar, the compressive stress-strain relationship of bare bar is used. Similarly, by combining the models of concrete and bar, the model of RC can be obtained.

The above constitutive models for axi-symmetric RC element are implemented into the existing "WCOMR" [7] which is a computer package for performing nonlinear finite element analysis of two dimensional reinforced concrete structures, and was written in FORTRAN language. It is noted that the package can be run by either a personal computer or a workstation.

3. VERIFICATION WITH EXPERIMENTAL RESULTS OF SMALL-SCALE SLABS

3.1 Tested Circular Slabs under Uniformly Distributed Load

A test of circular slab subjected to a uniformly distributed load which was performed by Iwaki et al., [6] is selected to check a reliability of the proposed constitutive models for axi-symmetric reinforced concrete structures. Dimension and reinforcement

arrangement of the tested slabs are illustrated in Fig.5. A reinforcement ratio of a stirrup p_v for each specimen is varied, i.e. p_v = 0, 0.1%, 0.2%, 0.4% and 0.65%, while the reinforcement ratios in the radial and hoop direction are fixed. It should be noted that the reinforcement ratio of the stirrup is taken at the 1.5d from the support (where d=9.5 cm, the effective height of the specimen). For the concrete, a compressive strength is 250 kgf/cm^2, and a tensile strength adopted in the present analysis is 20 kgf/cm^2. In addition, the yield strength of the reinforcing bars is 3,500 kgf/cm^2. The specimens are simply supported by a circular support and a uniformly distributed load is applied at the region inside the circular support.

In the nonlinear finite element analysis, the above-mentioned tested circular slab is discretized into a four node axi-symmetric finite element mesh, and due to a symmetry, only half of the slab is analyzed. Fig. 6 shows the finite element (FEM) mesh and loading condition.

3.2 Comparison between Experimental and Numerical Results

Nonlinear analyses of the RC circular slab for five cases of different ratios of stirrups by using WCOMR with the proposed constitutive models for axi-symmetric reinforced concrete structures are performed. The present nonlinear analysis can obtain the complete load-displacement curves up to the ultimate state for all specimen, i.e. A03 (p_v = 0), SG2D6 (p_v= 0.1%), SG2D5 (p_v= 0.2%), SG2D4 (p_v = 0.4%), SG2D3 (p_v = 0.65%). Fig.7a-7c show the comparison of load-displacement curves in cases of p_v = 0, 0.1% and 0.65%. The ultimate loads of all specimens are tabulated in Table 1. For the results of cracking patterns, Fig.8 shows a typical example in case of the specimen SG2D6 (p_v = 0.1%).

From the comparison in Fig.7a-7c, the nonlinear behaviors of the tested specimens are predicted reasonably well, although the initial stiffnesses of the load-displacement curves are different between the numerical and experimental results due to over-estimation of an elastic modulus of concrete in the present analysis. A yielding point obtained by the numerical analysis of each case coincides with test results. As shown in Fig.7b and 7c for the specimens with stirrups, the yielding plateaus of the load-deformation curves are obtained, however, the remarkable strain-hardening behaviors cannot be simulated. This might be due to the fact that the approximated bilinear constitutive model of reinforcing bars in considered in the adopted model [7].

As can be seen from the comparison of ultimate loads tabulated in Table 1, all numerical results are lower than the experimental ones. The differences between experimental and numerical results are in the range of 4.4% to 16.5% for the specimens with varied stirrup ratios from 0% to 0.65%, and the difference becomes larger while the stirrup ratio is increased. This might be because the hardening portion of the reinforcing bar model is excluded in the analyses as explained above.

As shown in Fig.8, for a typical case of the specimen SG2D6 (p_v = 0.1%), the crack pattern obtained in the present numerical results has the same tendency as the tested results. Shear punching failure is the predominant failure pattern, which is identical with the tested results, and the first failure element located at 14.5 cm from the support on the upper surface as shown in Fig.8, coincides well with that obtained from the experimental result (1.5d = 14.25 cm from the support on the upper surface). Therefore, from the above comparison between the experimental and numerical results, it can be concluded that the present analytical procedure can be used to simulate the behavior of the tested RC circular slabs subjected to a uniformly distributed load up to the failure of the structures.

4. VERIFICATION WITH FULL-SCALE TEST RESULTS OF MASSIVE SLABS

The large-scale axi-symmetric reinforced concrete structure, i.e., the bottom slab of the liquefied natural gas inground storage tank with a thickness of 7 meter and a radius of 33.7 meter, is selected in order to show the applicability of the proposed analytical procedure to the real structure. This structure has been designed and constructed in Japan, and now under operation. When the construction of this tank has been completed, the pressure load test on the bottom slab was performed and all important data were recorded. The uplift water pressure loaded on the bottom face of the slab is increased gradually until the design level of 40.6 tf/m^2.

As shown in Fig.9, the bottom slab structure is discretized into finite element mesh consisting of four-node axi-symmetric elements with the appropriate boundary conditions including the subgrade reactions of ground beneath the bottom slab, and the connection point between the bottom slab and a side wall.

In order to simulate the behavior of the tested slab, the parametric studies on the concrete strength are performed. It is noted that other parameters such as yield strength of bars etc., are kept constants. The reason to select only the concrete strength as the parameter is that the concrete material properties are less reliable than the steel, and since the main objective of this study is to investigate the behavior of RC structure alone, despite uncertainties in subgrade reaction springs and connection springs, their properties are kept constant.

From the present numerical results, the relations between a vertical displacement at the center (R=0, where R: a radial distance from the center) and a water pressure are plotted in Fig.10 for the above three cases of different values of concrete strength, i.e.

- $0.7\ f_t$ and $0.9\ f'_c$
- $0.8\ f_t$ and $0.9\ f'_c$
- $1.0\ f_t$ and $1.0\ f'_c$

where

f'_c : cylinder compressive strength

f_t : tensile strength (from splitting test or equivalent)

The comparison among these results and the experimental ones shows that the numerical results give larger displacement, and hence they seems to be softer than the experimental ones. At the design load level, the differences of numerical results for all three cases and the experimental results are approximately less than 7% which is practically acceptable.

For the relation of rebar stress and water pressure, Fig.11 shows the radial rebar stress at the center (R = 0), and Fig.12 shows the inclined rebar stress at the point of discontinuity in slab thickness (R = 30.23m). By comparing the numerical results with the experimental ones in Fig.11, 12, it was found that at the design load level, the numerical results for the case of $0.7\ f_t$, $0.9f'_c$ give the closest results in comparison with the experimental ones, and the difference for this case is approximately less than 9%, which is again acceptable.

Hence, by considering both comparisons of displacement and rebar stresses, the case of $0.7\ f_t$, $0.9\ f'_c$ is the most appropriate model for simulating the behavior of the slab up to the design load level.

5. CONCLUDING REMARKS

This paper presents the nonlinear analyses of reinforced concrete axi-symmetric structures using simplified constitutive models. The concept of the proposed model applied for a cracked reinforced concrete axi-symmetric element is the superposition between two independent models, i.e. two-dimensional model in the plane of raidal and vertical

direction, and one-dimensional model in the hoop direction. The constitutive models for each of the above two models developed by Okamura and Maekawa are employed in the present study. The existing nonlinear finite element program called "WCOMR" is modified to incorporate the proposed axi-symmetric model.

Through the comparison with the results of the test on circular slabs under a uniformly distributed load with different cases of stirrup ratios, the verification of present numerical analysis is made.

By using the proposed analytical procedure, the nonlinear analyses of a real massive bottom slab of LNG inground storage tank is performed. Good agreement between the full-scale test and the numerical results data up to design load stage is obtained.

Therefore, the present nonlinear analysis method can be used as a tool for the prediction the behavior of the large-scale axi-symmetric reinforced concrete structures, which could be hardly performed by the experiment in a true scale.

6. ACKNOWLEDGMENT

The author is pleased to acknowledge Obayashi Corporation, Tokyo, Japan, for supporting this research work. He also expresses his deepest appreciation to Prof. K. Maekawa, the University of Tokyo for the continuous suggestion and cooperation, and thanks to Mr. Bing Wang for helping computional works.

7. REFERENCES

1. Mackerle, J., Finite and Boundary Element Analyses of Concrete and Concrete Structures - A Bibliography (1991-1993), *Finite Elements in Analysis and Design.* Vol. 16, 1994, pp 71-83.
2. Cheung, M.S. and Li, W., Finite Strip Method for Materially Nonlinear Analysis of Reinforced Concrete Slab, *Computers and Structures,* Vol. 35, No. 5, 1990, pp. 603-607.
3. Rangan, B.V., Flexural Design of Reinforced Concrete Slabs in accordance with AS 3600, *Transactions of the Institution of Engineers, Australia,* Civil Engineering, Vol. CE31, No. 2, July 1989, pp. 79-85.
4. Shehata, A. E. and Regan, P.E., Punching in R.C. Slabs, *Journal of Structural Engineering,* Vol. 115, No.7, July 1989, pp. 1726-1740.
5. Zhou, K.R. and Jian, D.H., Imitation of Punching Failure for Reinforced Concrete Slabs in Finite Element Method, *Proceedings of the Asian Pacific Conference on Computational Mechanics,* Hong Kong, December 1991.
6. Iwaki R., Akiyama, H., Okada, T. and Shioya, T., Shear Strength of Reinforced Concrete Circular Slabs, *Proceedings of Japan Society of Civil Engineers,* No. 360/V-3 (Concrete Engineering and Pavements), August 1985.
7. Okamura, H. and Maekawa, K., *Nonlinear Analysis and Constitutive Models of Reinforced Concrete,* Giho-do Press, Tokyo, Japan, 1991.
8. Shima, H., Chou, L.L. and Okamura, H., Micro and Macro Models for Bond Behavior in Reinforced Concrete, *Journal of the Faculty of Engineering, University of Tokyo (B),* Vol. 39, No. 2, 1987.
9. Izumo, J., Shima, H. and Okamura, H., Analytical Model for RC panel Elements Subjected to In-plane Forces, *Concrete Library International, JSCE,* No. 12, 1989.
10. Maekawa, K. and Okamura, H., The Deformational Behavior and Constitutive Equation of Concrete Using Elasto-Plastic and Fracture Model, *Journal of*

Faculty of Engineering, University of Tokyo (B), Vol. 37, No. 2, 1983.

11. Okamura, H. *Limit States Design Procedure of Reinforced Concrete Structure,* Kyotachi Press, Japan 1991 (in Japanese).

Table 1 Comparison of the ultimate loads and failure positions for different cases of the reinforcement ratio of stirrup

	No. of Specimen	A03 (p_v = 0)	SG2D6 (p_v = 0.1%)	SG2D5 (p_v = 0.2%)	SG2D4 (p_v = 0.4%)	SG2D3 (p_v = 0.65%)
Experimental results	Failure position (from support)	1.5d = 14.25cm	1.5d = 14.25cm	1.5d = 14.25cm	1.5d = 14.25cm	1.5d = 14.25cm
	Ultimate load (kgf/sq.cm)	7.06	10.6	12.74	12.78	13.23
Numerical result	Failure position (from support)	14.5cm	14.5cm	14.5cm	14.5cm	14.5cm
	Ultimate load (kgf/sq.cm)	6.75	9.80	10.6	10.81	11.05
Difference	Ultimate load (%)	4.4	7.5	16.8	15.4	16.5

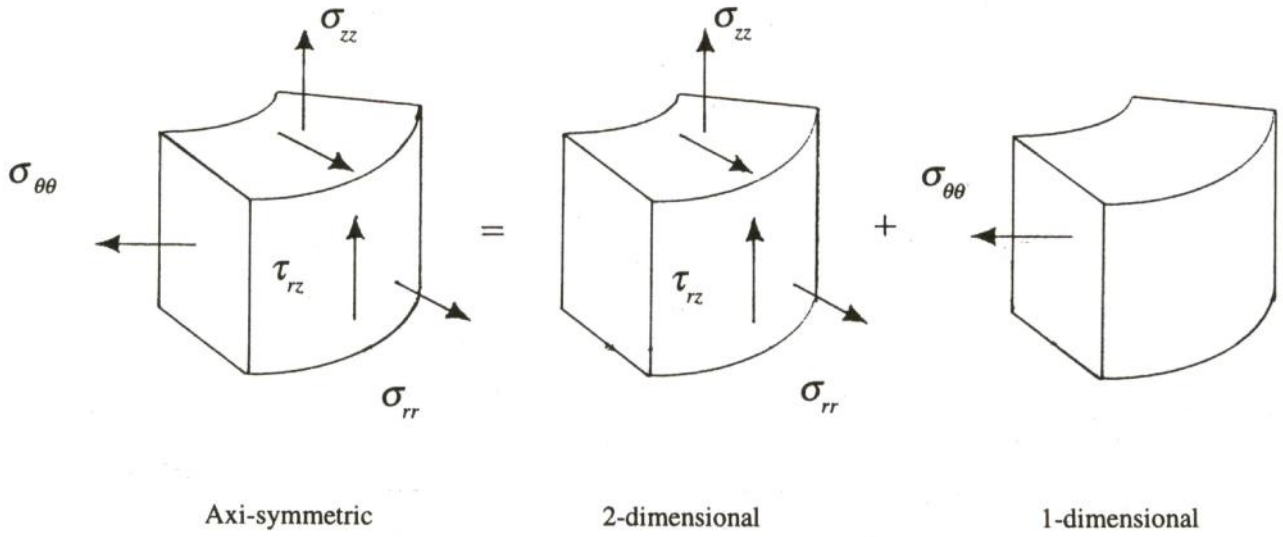

Fig. 1 Constitutive model for axi-symmetric RC element after cracking

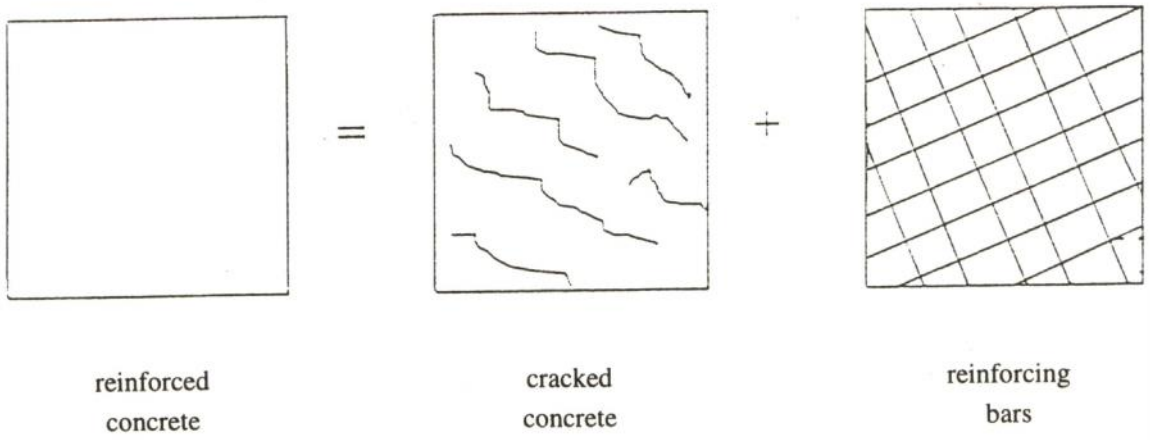

Fig. 2a Composition of reinforced concrete (RC) plate element model (from Ref. [7])

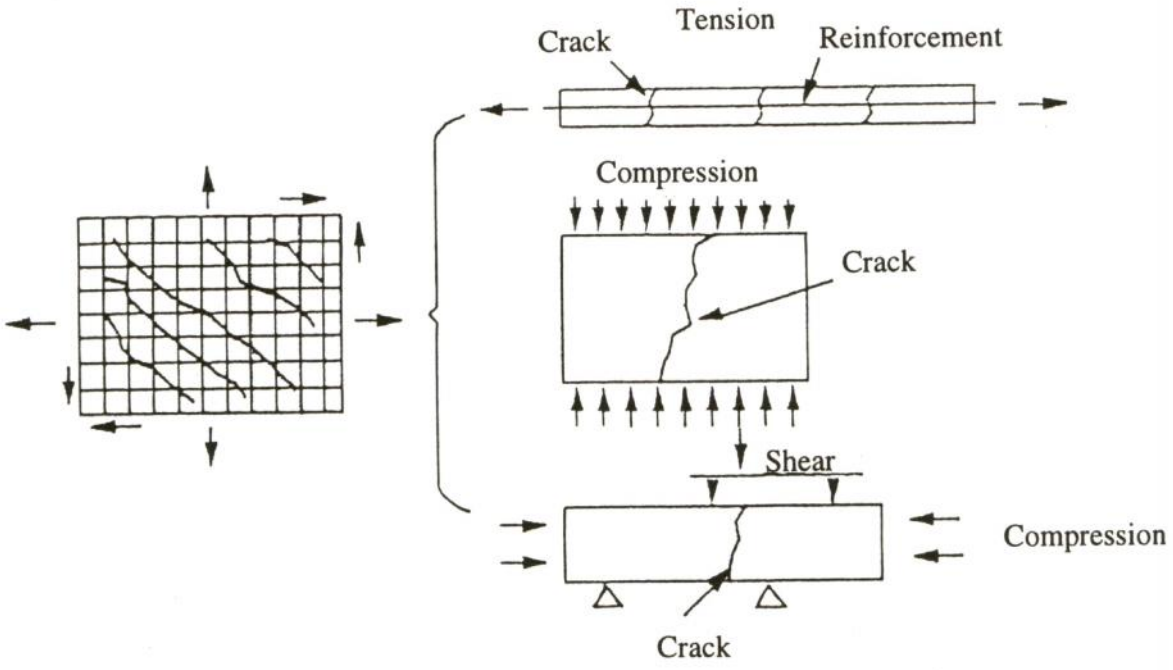

Fig. 2b Construction fo cracked concrete model (from Ref. [7])

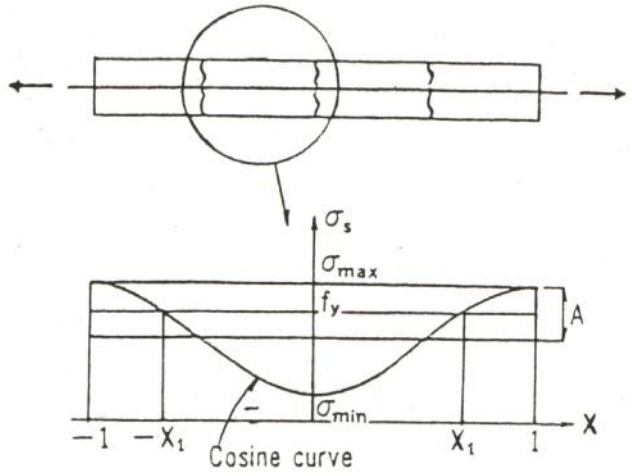

Fig. 3a Assumption for stress distribution of bars in concrete (from Ref. [7])

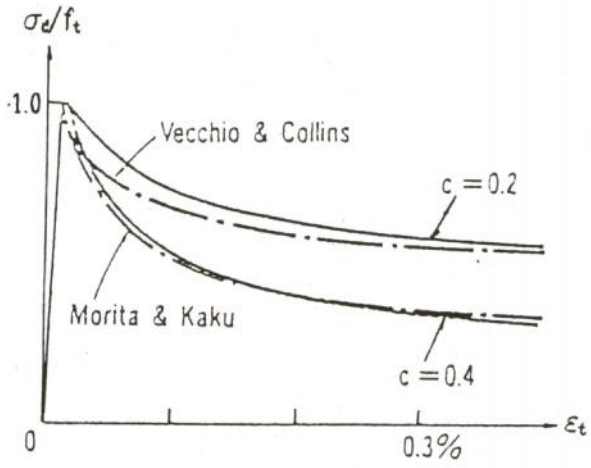

Fig. 3b Tension stiffening model for deformed bars (c = 0.4) and for welded meshes (c = 0.2) (from Ref. [7])

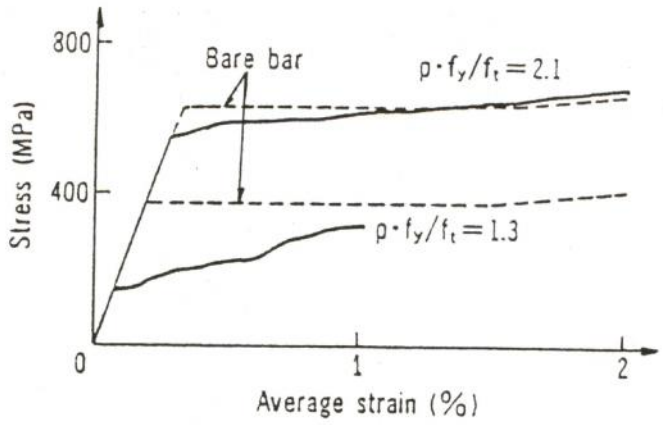

Fig. 3c Example of average stress-average strain of bar in concrete (from Ref. [7])

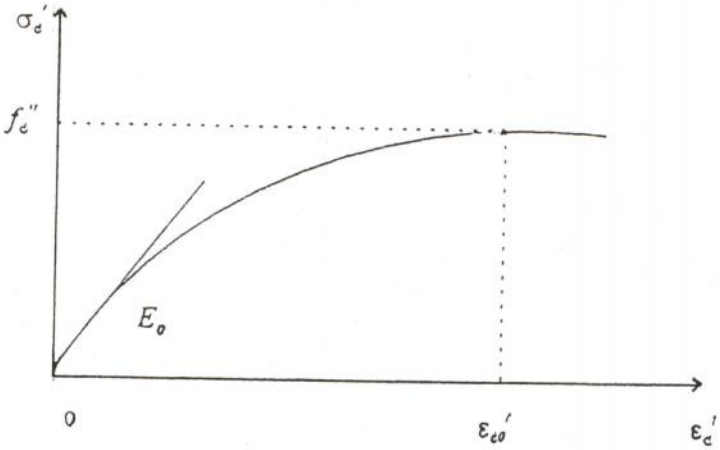

Fig. 4 Compressive stress-strain of concrete

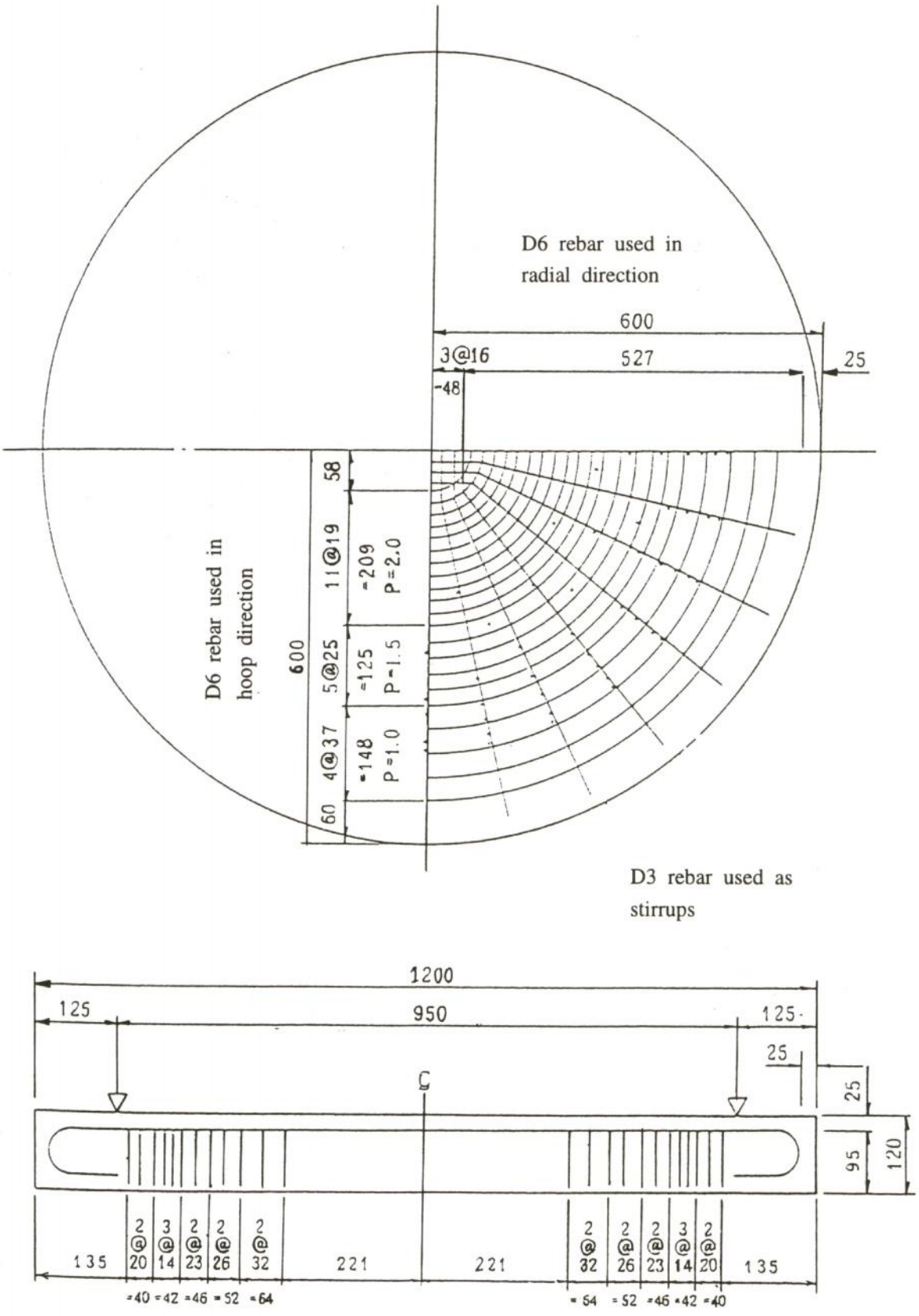

Fig. 5 Dimension, support condition and reinforcement arrangement of test specimen SG2D6 (p_v = 0.1%)

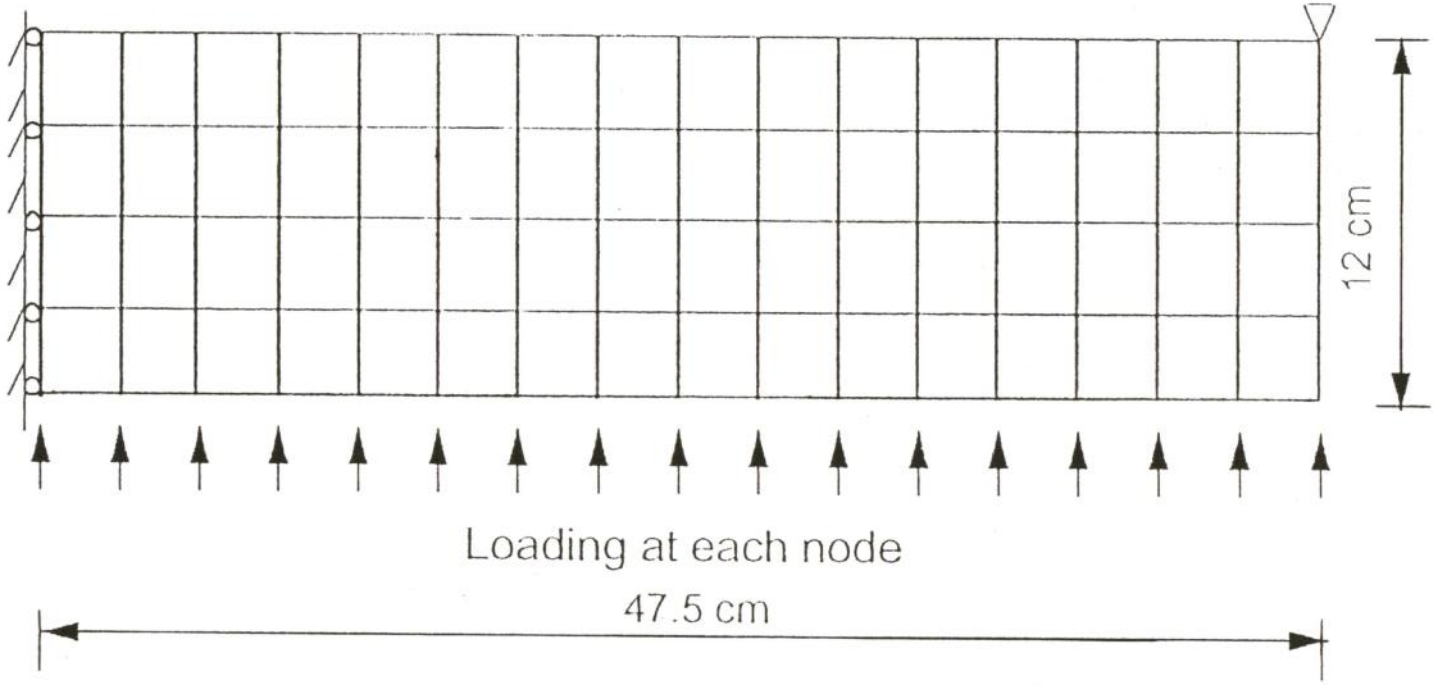

Fig. 6 FEM mesh and loading condition of circular slab

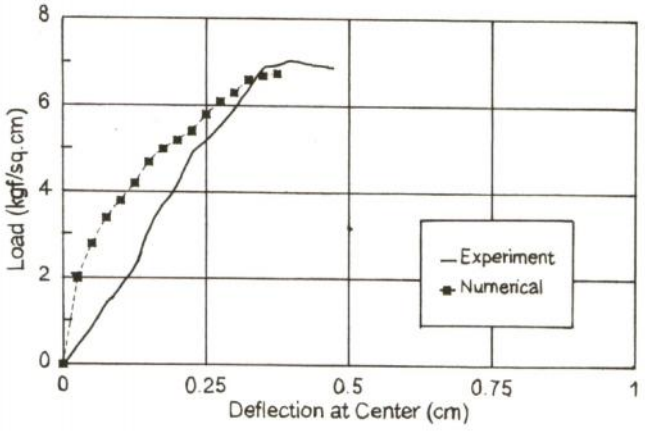

Fig. 7a Comparison between experimental and numerical results Specimen A03 (p_v=0)

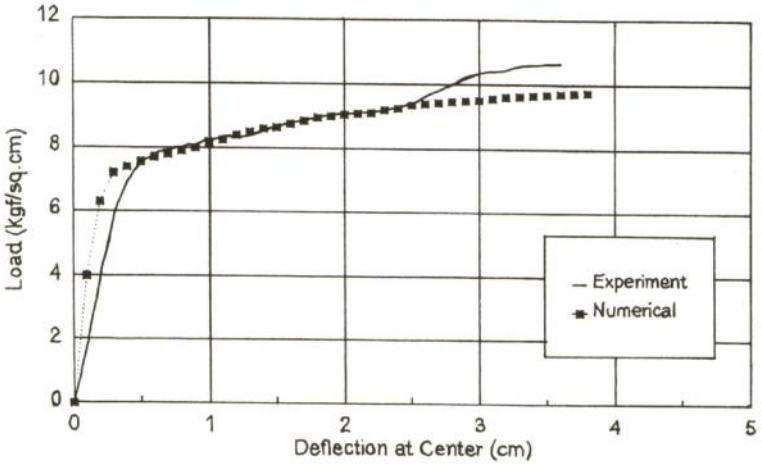

Fig. 7b Comparison between experimental and numerical results Specimen SG2D6 (p_v=0.1%)

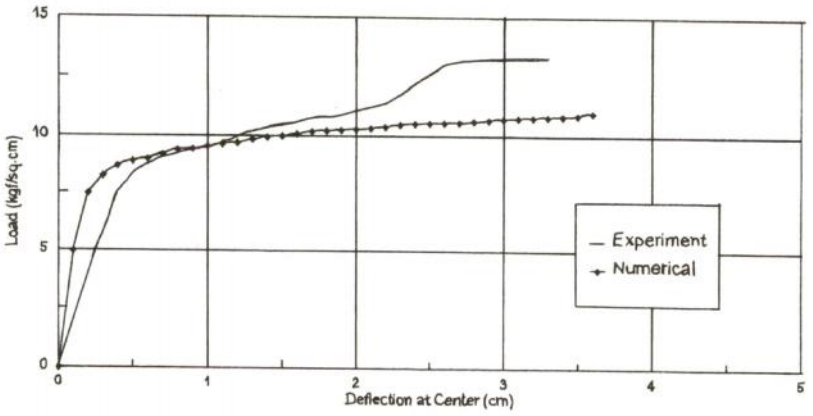

Fig. 7c Comparison between experimental and numerical results Specimen SG2D3 (p_v=0.65%)

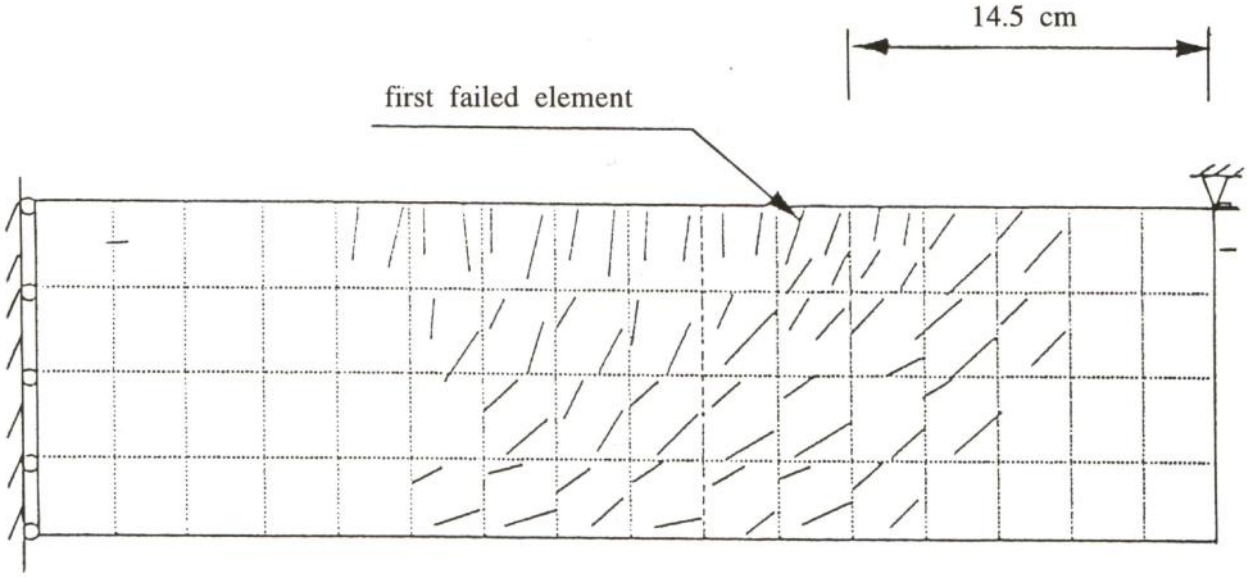

numerical

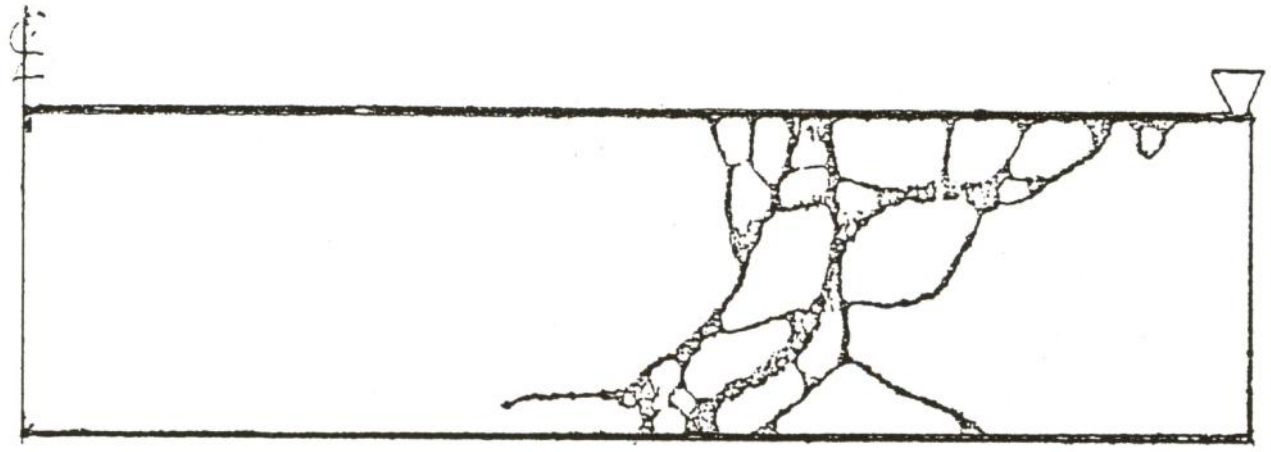

experimental [6]

Fig. 8 Cracking pattern for the specimen SG2D6 (p_v=0.1%)

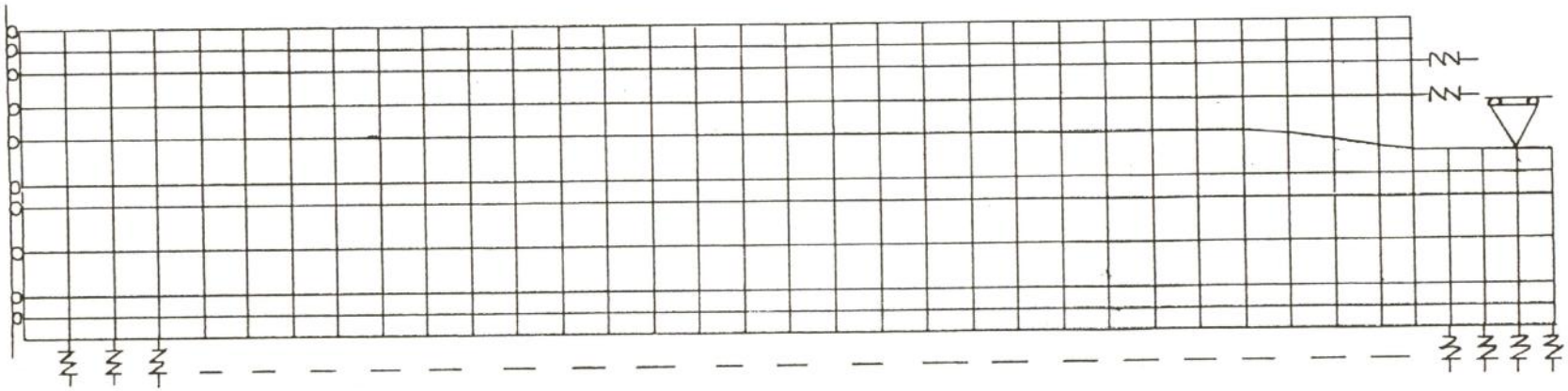

Fig. 9 Finite element mesh and boundary condition of bottom slab of LNG tank

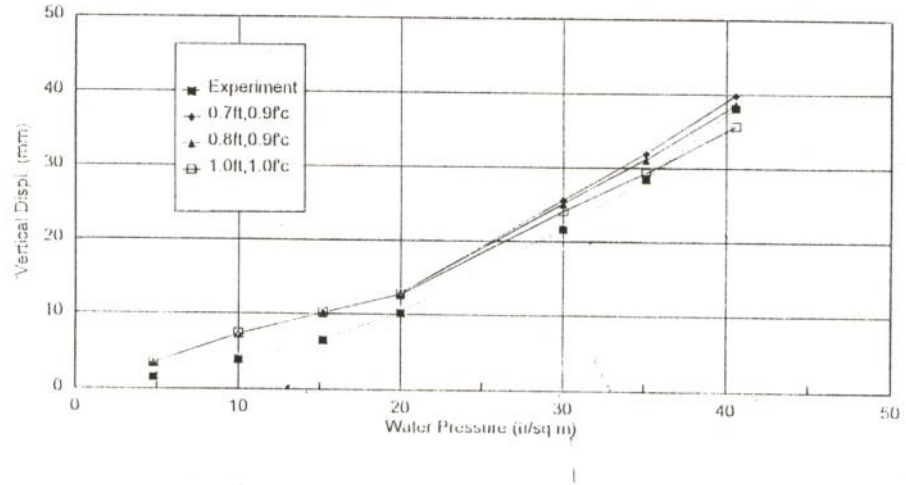

Fig. 10 Relation between vertical displacement and water pressure at R=0

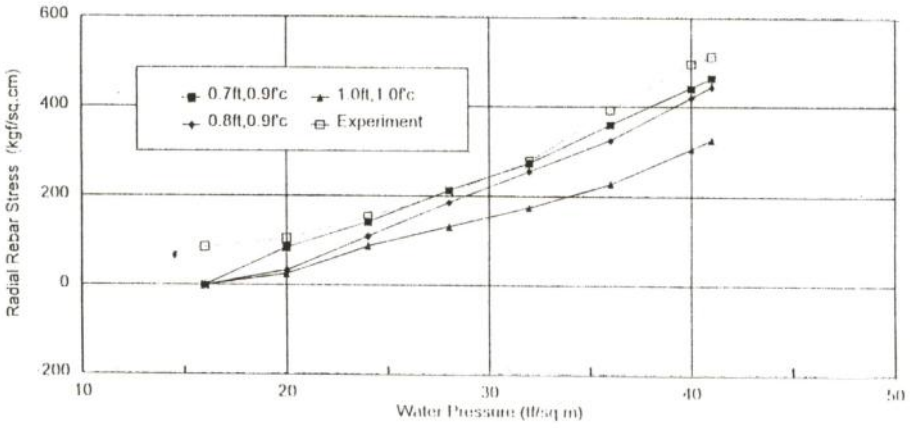

Fig. 11 Relation between radial rebar stress and water pressure at R=0

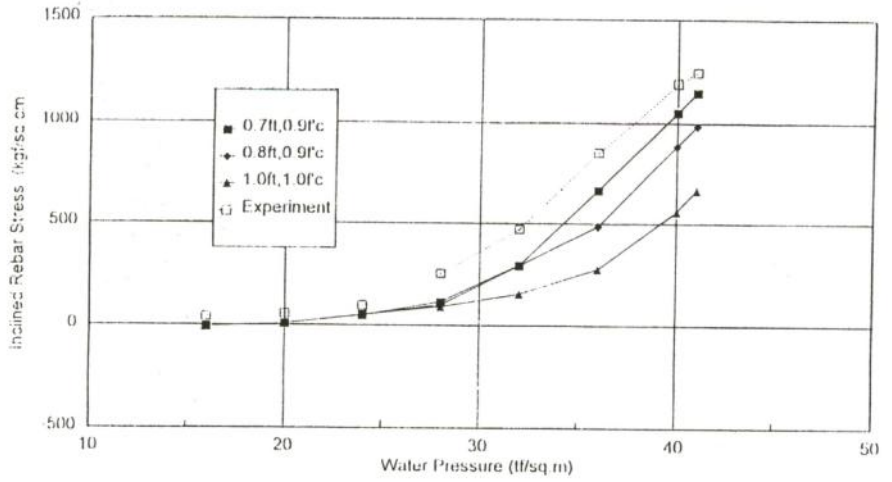

Fig. 12 Relation between inclined rebar stress and water pressure at R=30.23 m